Antibody-lectin chimeras for glyco-immune checkpoint blockade

Jessica C. Stark[1,*], Melissa A. Gray[1,*], Simon Wisnovsky[2], Itziar Ibarlucea-Benitez[3], Nicholas M. Riley[1], Mikaela K. Ribi[1], Marta Lustig[4], Wesley J. Errington[5], Bence Bruncsics[6], Casim A. Sarkar[5], Thomas Valerius[4], Jeffrey V. Ravetch[3], Carolyn R. Bertozzi[1,7]

[1]Department of Chemistry and Sarafan ChEM-H, Stanford University, Stanford, CA, USA

[2]Faculty of Pharmaceutical Sciences, University of British Columbia, Vancouver, BC, Canada

[3]Laboratory of Molecular Genetics and Immunology, The Rockefeller University, New York, NY, USA

[4]Division of Stem Cell Transplantation and Immunotherapy, Department of Medicine II, Christian Albrechts University Kiel and University Medical Center Schleswig-Holstein, Kiel, Germany

[5]Department of Biomedical Engineering, University of Minnesota, Minneapolis, MN, USA

[6]Department of Measurement and Information Systems, Budapest University of Technology and Economics, Budapest, Hungary

[7]Howard Hughes Medical Institute, Stanford, CA, USA

[*]J.C.S. and M.A.G. contributed equally

Abstract

Despite the curative potential of checkpoint blockade immunotherapy, a majority of patients remain unresponsive to existing treatments. Glyco-immune checkpoints – interactions of cell-surface glycans with lectin, or glycan binding, immunoreceptors – have emerged as prominent mechanisms of immune evasion and therapeutic resistance in cancer. Here, we describe antibody-lectin chimeras (AbLecs), a modular platform for glyco-immune checkpoint blockade. AbLecs are bispecific antibody-like molecules comprising a tumor-targeting arm as well as a lectin "decoy receptor" domain that directly binds tumor glycans and blocks their ability to engage lectin

receptors on immune cells. AbLecs elicited tumor killing *in vitro* via macrophage phagocytosis and NK cell and granulocyte cytotoxicity, matching or outperforming combinations of monospecific antibodies with lectin-blocking or glycan-disrupting therapies. Furthermore, AbLecs synergized with blockade of the "don't eat me" signal CD47 for enhanced tumor killing. AbLecs can be readily designed to target numerous tumor-associated antigens and glyco-immune checkpoint ligands, and therefore represent a new modality for cancer immune therapy.

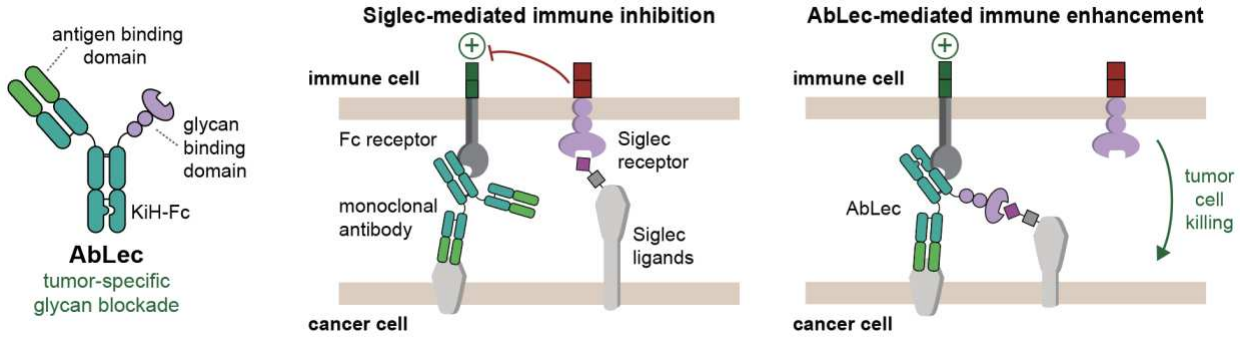

Graphical Abstract. Antibody-lectin chimeras for glyco-immune checkpoint blockade

Introduction

T cell checkpoint blockade immunotherapies (e.g., PD-1/PD-L1 or CTLA-4 targeting antibodies) are now used to treat nearly half of all cancer patients in the US[1]. However, these therapies are effective in only a small fraction (<20%) of treated patients[1] and, of those who respond, at least 25% will develop resistance[2]. Thus, there is an urgent need for therapies targeting additional immune checkpoints that drive cancer progression.

Altered cell surface glycosylation is a hallmark of cancer that is associated with poor disease prognosis[3–5]. These altered glycan structures mediate immune modulation through interactions with lectin (glycan-binding) immunoreceptors, including sialic acid-binding immunoglobulin-like lectins (Siglecs)[6], selectins[7], and galectins[8]. In particular, multiple recent

studies indicate that upregulation of cell-surface sialoglycans allows tumors to engage inhibitory Siglec receptors on immune cells and evade immune surveillance[9–17]. Taken together, glyco-immune checkpoints are emerging as attractive targets for cancer immunotherapy.

However, multiple challenges have historically prevented therapeutic targeting of glyco-immune checkpoints in cancer (**Fig 1a**). The weak immunogenicity of mammalian glycan structures can undermine the development of specific and high-affinity anti-glycan antibodies. To put this in perspective, a recent report cataloged 417 commercially available antibodies targeting glycans[18]. The same study noted that a single supplier offers 287 unique antibodies to tubulin and 269 unique antibodies to CD4, meaning that there are more antibodies to these two proteins available from a single supplier than all the commercially available anti-glycan antibodies combined. Further complicating monoclonal antibody development is the fact that many lectin receptors have multiple ligands that are expressed in the context of cancer[9,14], and often the precise identities of their ligands are unknown. “Decoy receptor” molecules composed of a lectin glycan-binding domain fused to an antibody Fc domain address this complexity by retaining native glycan-binding specificities; however, their low binding affinities (typically with K_Ds in the μM to mM range[19]) preclude their use as therapeutics.

We recently developed enzyme conjugates for targeted degradation of glycans[11,15] or glycoproteins[20] as an alternative approach to potentiate anti-tumor immunity, but these molecules require substantial engineering to target new types of glycans. In addition, such approaches are currently restricted to degradation of broad classes of glycans (e.g., sialoglycans[11,15]) or glycoproteins (e.g., mucins[20]), rather than the specific molecules involved in immune regulation. Finally, while lectin-targeted blockade antibodies such as those directed against galectin-9[21] and Siglec-15[22] are being tested in the clinic, these untargeted checkpoint blockade reagents are likely to elicit immune-related adverse events, which are observed in at least 50% of patients treated with existing checkpoint blockade immunotherapies[23]. In contrast, tumor-targeted immunotherapies (e.g., monoclonal antibodies targeting tumor-associated antigens) generally

offer improved safety profiles[24]. Overall, our inability to specifically and directly block immunomodulatory glycans on tumors, even after development of multiple therapeutic modalities, highlights the significance of this technological gap.

Here, we describe antibody-lectin (AbLec) chimeras as a modular approach to target glycans for cancer immunotherapy. AbLecs couple low affinity glycan binding domains from lectin receptors to high affinity antibodies targeting tumor antigens (**Fig. 1a**). This approach uniquely enables blockade of inhibitory tumor glycans at nanomolar concentrations agnostic of their specific identities. We show that AbLecs enhance killing of tumor cell lines *in vitro* compared to the parent tumor-targeting antibody by donor-derived macrophages, natural killer (NK) cells, and granulocytes. AbLecs outperformed combination of a tumor-targeting antibody and a lectin receptor-blocking antibody, suggesting there is a therapeutic benefit to targeting glycans directly. Further, we found that AbLec treatment was synergistic with blockade of the “don’t eat me” signal CD47, indicating that glyco-immune checkpoint blockade has the potential to work in combination with existing classes of cancer immunotherapies. Finally, we show that the AbLec platform can be applied to target diverse tumor-associated antigens, including HER2, CD20, and EGFR, as well as multiple classes of immunomodulatory glycans, such as the ligands for established Siglec[12,14,25,26] and galectin[27] checkpoints. Overall, AbLecs represent a generalizable approach for glyco-immune checkpoint blockade and a new modality for cancer immunotherapy.

Results

AbLecs bind to targeted cells at nanomolar concentrations

We hypothesized that high-affinity binding of an antibody Fab domain to tumor antigens would allow AbLecs to accumulate at sufficiently high local concentrations so as to permit binding of a relatively low affinity lectin domain to inhibitory glycans on the same cell. As proof-of-concept, we created AbLecs that combine an Fab domain from trastuzumab, an FDA-approved monoclonal

antibody that binds the tumor antigen HER2, with the extracellular domains of Siglec-7 or -9 fused to an Fc domain. We used a modified knobs-into-holes[28] Fc engineering approach to facilitate self-assembly of heterotrimeric AbLecs in a single expression culture (**Fig. 1b**). Indeed, coexpression of trastuzumab heavy and light chains with Siglec-7-Fc or Siglec-9-Fc in Expi293 cells resulted in expression of single protein products (**Fig. 1c**). Reducing SDS-PAGE analysis showed that trastuzumab x Siglec-7 (T7) and trastuzumab x Siglec-9 (T9) AbLecs were composed of 3 disulfide bonded protein chains consistent with the molecular weights of the Siglec-Fc and the trastuzumab heavy and light chains (**Fig. 1c**). Western blotting against HA and His_6 tags on the Siglec-Fc and antibody heavy chains, respectively, further demonstrated that full-length AbLecs are composed of both antibody and decoy receptor arms (**Fig. 1d**), which was confirmed by mass spectrometry (**Supplementary Fig. 1**).

We next characterized binding of T7 and T9 AbLecs to HER2+ cell lines compared to trastuzumab and Siglec-Fc decoy receptor controls. Dissociation constant (K_D) values for T7 and T9 AbLecs were measured by quantifying binding to SK-BR-3 cells at various concentrations via flow cytometry. SK-BR-3 cells express the HER2 antigen bound by trastuzumab as well as ligands for Siglecs-7 and -9, as assessed by flow cytometry (**Fig. 1e**). As expected, the decoy receptor controls (Siglec-7/9-Fc) bind only at low levels to SK-BR-3 cells, even at the highest concentrations tested (200 nM) and despite the fact that SK-BR-3 cells express Siglec-7 and -9 ligands (**Fig. 1f**). However, by combining the decoy receptor arm with the high affinity trastuzumab antibody arm, AbLecs bind to SK-BR-3 cells with K_D values in the low nM range, similar to that of the parent bivalent antibody trastuzumab (**Fig. 1g**). Thus, AbLecs enable recruitment of otherwise low affinity lectin binding domains to cell surfaces at nanomolar concentrations.

Despite the low affinity of the Siglec domain in comparison to the antibody arm, AbLec binding affinity is governed by both components. By mutating a conserved arginine residue in the Siglec-Fc binding site to an alanine, we created T7A and T9A AbLec mutants that exhibit significantly reduced affinities for Siglec ligands, as previously reported[29]. The mutant AbLecs

exhibited reduced binding to SK-BR-3 cells, and resulted in a ~2-3-fold increase in apparent K_D compared to WT AbLecs (**Supplemental Fig. 2a-c**).

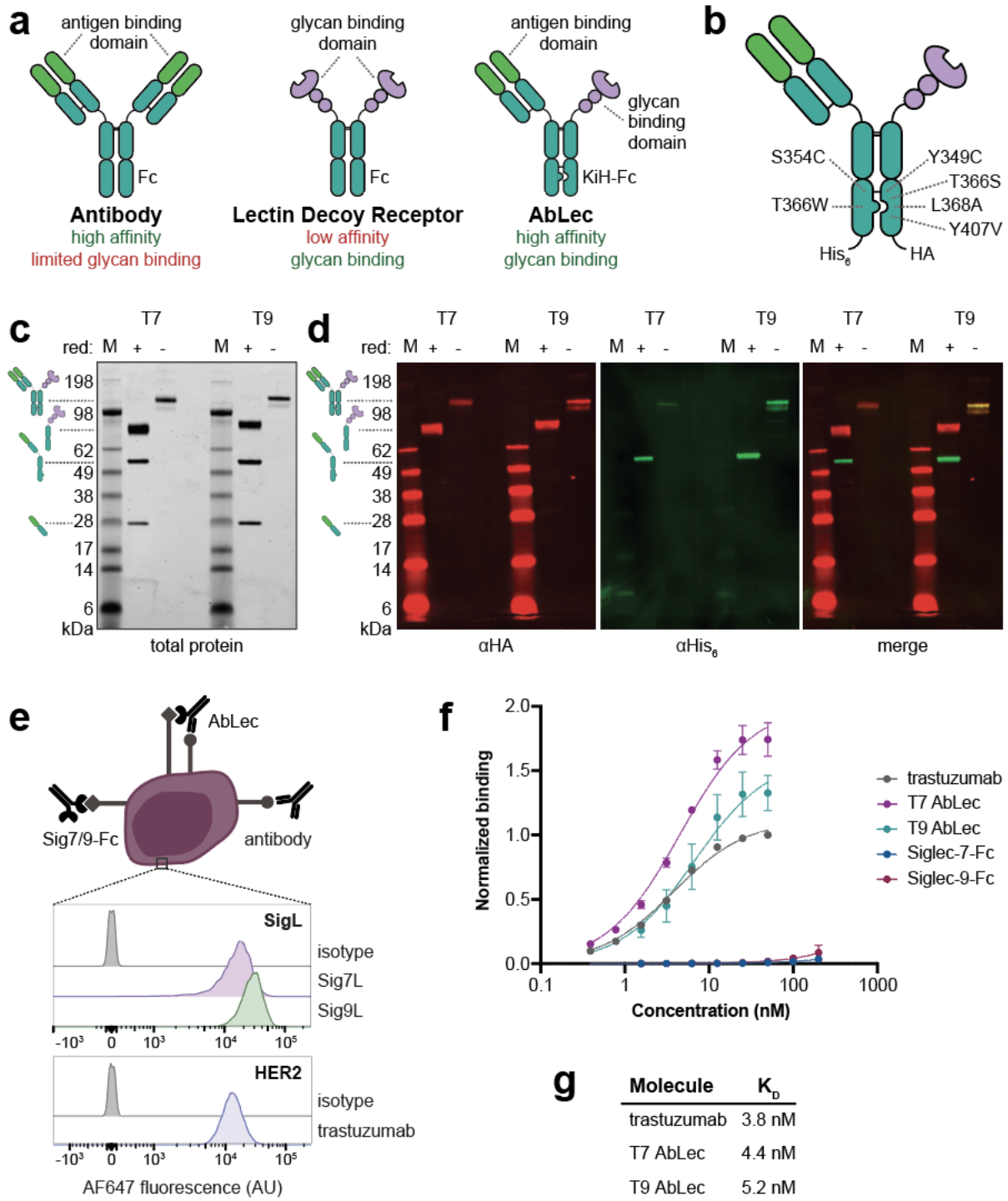

Figure 1. AbLecs enable use of lectin decoy receptors for glyco-immune checkpoint blockade.

(**a**) AbLecs couple high affinity, tumor-targeting antibodies to low affinity glycan binding domains from lectin immunoreceptors.

(**b**) Fc engineering based on established knobs-into-holes technology in a human IgG1 antibody framework facilitates self-assembly of antibody-lectin chimeras.

(**c**) SDS-PAGE analysis of T7 and T9 AbLecs shows that AbLecs are composed of 3 disulfide bonded protein chains consistent with the molecular weights of Siglec-Fc, antibody heavy chain, and antibody light chain (total protein gel). Under non-reducing conditions, T7 and T9 AbLecs run as a single protein product. Gel is representative of n = 3 biological replicates.

(**d**) Western blot detection of antibody heavy chain (αHis_6) and Siglec-Fc chains (αHA) revealed that AbLecs are composed of antibody and Siglec decoy receptor arms. Blots are representative of n = 3 biological replicates.

(**e**) SK-BR-3 cells express the HER2 antigen bound by trastuzumab as well as ligands for Siglec-7 and -9 (Sig7L and Sig9L, respectively). Flow cytometry plots are representative of n = 3 biological replicates.

(**f**) Binding of T7 AbLec, T9 AbLec, trastuzumab, Siglec-7-Fc, and Siglec-9-Fc to SK-BR-3 cells was quantified via flow cytometry (n = 3, binding normalized to 50 nM trastuzumab for each experimental replicate).

(**g**) Dissociation constants for trastuzumab, T7, and T9 AbLecs determined by fitting experimental data to a one-site total binding curve.

We further interrogated the mechanism of AbLec binding via a structure-guided computational modeling approach[30]. We used the recently developed *MVsim* toolset[31] to construct a computational model of T7 AbLec binding trained using our experimental data (**Supplemental Fig. 2d**). Our computational model estimated that the apparent concentration of Siglec-7 ligands on the tumor cell surface was >2 orders of magnitude higher than that of the HER2 antigen (**Supplemental Fig. 2e**; $[HER2]_{app}$ = 0.2 μM; $[Sig7L]_{app}$ = 27 μM), suggesting that this abundance of accessible glycan ligands offsets the low monovalent Siglec domain affinity and facilitates cooperative AbLec binding. This observed contribution of the Siglec-Fc arm to binding may explain why AbLec dissociation constants are of the same order of magnitude as the bivalent parent antibody trastuzumab, despite having only one antibody arm.

Selective blockade of lectin receptor binding epitopes

We next asked whether AbLecs could successfully block engagement of their targeted glycan ligands by competing with lectin receptors. Toward this end, we tested the ability of T7 and T9 AbLecs to compete with fluorescently-labeled Siglec decoy receptors for binding to HER2+

K562 cells. This cell line expresses higher levels of ligands for Siglecs-7 and -9 compared to the targeted antigen HER2, offering a challenging target for glycan blockade (**Fig. 2a**). Both T7 and T9 AbLecs bound to HER2+ K562 cells with low nanomolar K_D values (**Supplemental Fig. 3**). We observed that treatment of cells with T7 or T9 AbLec diminished binding of fluorescently labeled Siglec-7 or Siglec-9, respectively, by flow cytometry (**Fig. 2b, c**). AbLecs reduced Siglec-Fc binding nearly to the level of sialidase treatment, suggesting that they are able to block the majority of glycan-dependent binding of Siglec receptors to cells (**Fig. 2b, c**). AbLecs further selectively block binding of the targeted lectin. Treatment with the T7 AbLec was able to block binding of the cognate Siglec-7-Fc to a greater extent than trastuzumab or the non-cognate T9 AbLec at all concentrations tested (**Fig. 2d**).

We were curious to know whether AbLecs block the same epitopes bound by their cognate lectin receptors. We recently reported that the predominant ligand for Siglec-7 expressed on K562 cells is the sialomucin CD43[16]. Further, the MEM59 anti-CD43 antibody binds to the same sialylated epitope on CD43 that is bound by Siglec-7[29]. We thus tested the ability of AbLecs to compete with the MEM59 antibody for binding to HER2+ K562 cells. We observed that the T7 AbLec blocked binding of MEM59 to a greater extent than trastuzumab or the non-cognate T9 AbLec controls, suggesting that the T7 AbLec binds and blocks the same CD43 glycoform bound by the endogenous Siglec-7 immunoreceptor (**Fig. 2e**). Taken together, this evidence suggests that AbLecs selectively block engagement of the targeted lectin immunoreceptor by competing for the same binding epitopes.

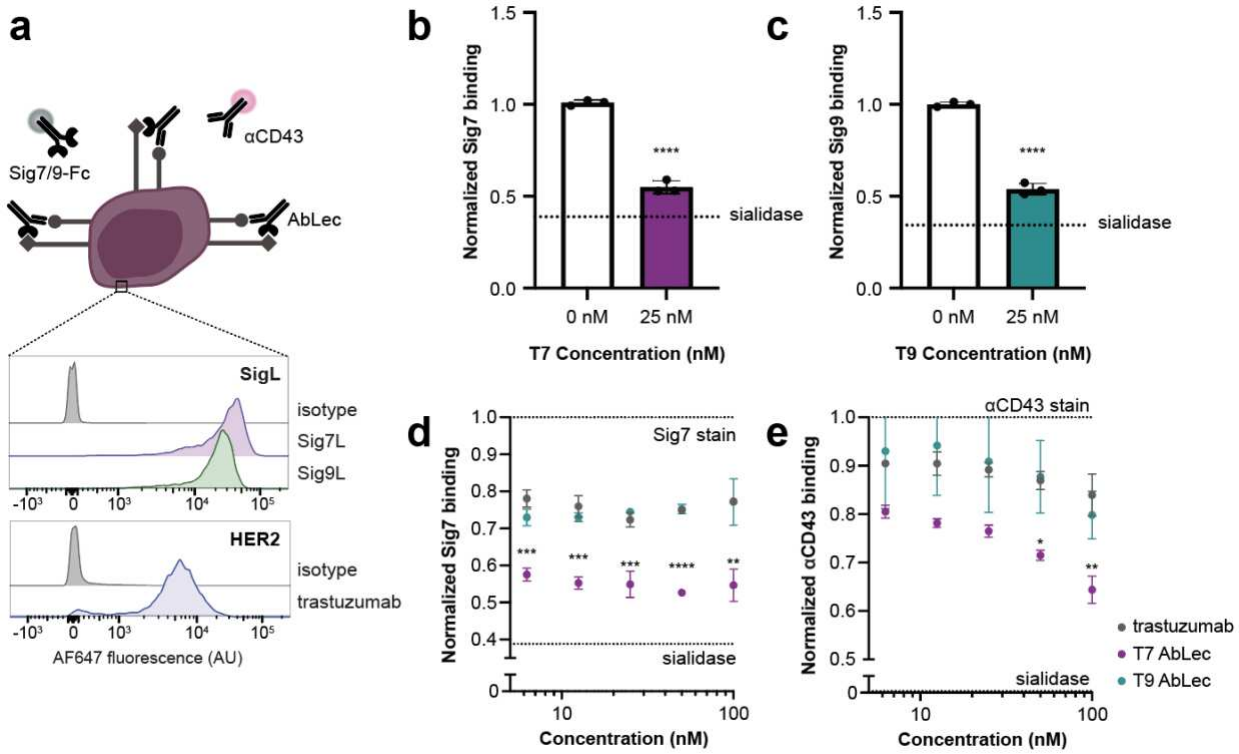

Figure 2. AbLecs selectively block lectin receptor binding epitopes.

(**a**) HER2+ K562 cells express the HER2 antigen bound by trastuzumab as well as ligands for Siglec-7 and -9 (Sig7L and Sig9L). Flow cytometry lots are representative of n = 3 biological replicates.

(**b, c**) T7 (**b**) or T9 (**c**) AbLec treatment blocks Siglec-7 or Siglec-9 receptor binding, respectively, in competitive binding assays with dye labeled Siglec-7 or -9-Fc (n = 3 biological replicates, normalized to Siglec-Fc staining with 0 nM AbLec).

(**d**) T7 AbLec, but not trastuzumab or T9 AbLec, blocks Siglec-7 receptor binding in competitive binding assays with dye labeled Siglec-7-Fc (n = 3 biological replicates, normalized to Siglec-7-Fc staining with 0 nM AbLec or antibody).

(**e**) T7 AbLec blocks binding of a αCD43 antibody that binds to the Siglec-7 receptor binding epitope in competitive binding assays with dye labeled αCD43 to a greater extent than trastuzumab or T9 AbLec (n = 3 biological replicates, normalized to αCD43 staining with 0 nM AbLec or antibody).

AbLecs potentiate tumor phagocytosis and cytotoxicity in vitro

Having demonstrated that AbLecs block binding of Siglec receptors to tumor cells, we tested whether AbLec treatment could enhance antibody-mediated tumor cell killing. Tumor targeting with antibody therapeutics creates an immune synapse between the targeted tumor antigen and antibody Fc receptors on the immune cells. Engagement of Fc receptors activates the immune cell to perform antibody effector functions (e.g., antibody-dependent cellular phagocytosis and antibody-dependent cellular cytotoxicity), which ultimately result in destruction

of the targeted tumor cell. However, Siglec ligands on the tumor cell surface recruit inhibitory Siglec receptors to the immune synapse, dampening immune cell activation and restricting antibody-mediated tumor cell killing[11,15]. In contrast, we hypothesized that AbLecs would block Siglec engagement at the immune synapse, mediating enhanced antibody effector functions (**Fig. 3a**).

We first tested this hypothesis using *in vitro* phagocytosis assays with primary human macrophages expressing Siglec-7 and -9 (**Supplemental Fig. 4**). We co-cultured macrophages with SK-BR-3 tumor cells labeled with a pH-sensitive dye that fluoresces red in acidic phagosomes, enabling quantification of phagocytosis via time lapse fluorescence microscopy. Images of macrophage/SK-BR-3 co-culture experiments after 5 h of incubation show that tumor cells treated with the T7 AbLec are more readily engulfed by macrophages into the low pH phagosome (indicated by red fluorescence) compared to those treated with the monospecific trastuzumab antibody or Siglec-7-Fc decoy receptor (**Fig. 3b**). Importantly, we did not observe any defects in cell growth or cytotoxicity over 72 hours of treatment with antibody, AbLec, or Siglec-Fc decoy receptors (**Supplemental Fig. 5**). We quantified the observed increase in phagocytosis using macrophages from three unique donors, and found that both T7 and T9 AbLecs significantly enhance phagocytosis of tumor cells compared to trastuzumab or Siglec-Fc decoy receptors alone (**Fig. 3c; Supplemental Fig. 6a**). We observed the same enhancement of phagocytosis in assays with the HCC-1854 and HER2+ K562 cell lines (**Supplemental Fig. 7a-d**).

We next asked whether AbLecs could enhance cell killing via the additional mechanism of antibody-dependent cellular cytotoxicity (ADCC). We co-cultured primary NK cells expressing Siglec-7 with SK-BR-3 tumor cells and analyzed cytotoxicity via flow cytometry (**Supplemental Fig. 8**). Across three unique donors, the T7 AbLec significantly enhanced NK cell cytotoxicity compared to trastuzumab or Siglec-7-Fc decoy receptor alone (**Fig. 3d; Supplemental Fig. 6b**). We observed the same effect in NK cell cytotoxicity assays with the HER2+ K562 cell line, which

expresses an order of magnitude lower levels of the targeted HER2 antigen and higher levels of Siglec-7 and -9 ligands, compared to SK-BR-3 cells (**Supplemental Fig. 7a, b, e**). We further investigated the potential for AbLecs to elicit cytotoxicity of SK-BR-3 cells mediated by polymorphonuclear granulocytes (PMNs) (**Supplemental Fig. 9**). We found that T7 and T9 AbLecs elicited increased tumor killing by PMNs compared to trastuzumab and AbLec isotype controls (**Supplemental Fig. 10a**).

AbLec mechanism of action is dependent on the bispecific molecular architecture and targeted glyco-immune checkpoint

We asked whether the chimeric AbLec architecture was required to potentiate tumor killing. To do this, we compared phagocytosis in macrophage/HER2+ K562 cell cultures treated with T7 AbLec or the combination of trastuzumab with the Siglec-7-Fc decoy receptor (**Fig 4a**). We found that combination of trastuzumab with Siglec-7-Fc did not enhance killing of HER2+ K562 cells compared to trastuzumab alone, as expected given the low binding affinity of the decoy receptor reagent (**Fig. 4b**). However, as before, treatment with T7 AbLec elicited enhanced tumor phagocytosis (**Fig. 4b**). From these results, we conclude that the chimeric AbLec architecture is required to recruit lectin decoy receptor domains to tumor cell surfaces at therapeutically relevant concentrations and potentiate tumor killing.

Critically, we tested whether AbLec-mediated enhancement of anti-tumor immune responses was a result of blockade of Siglec-glycan interactions. In these experiments, we pre-incubated macrophages or NK cells with Siglec-7 or -9 blocking antibodies prior to co-culture with SK-BR-3 cells (**Fig. 4c, top**). If the targeted Siglec receptor was blocked, tumor killing upon AbLec treatment was reduced to similar levels as those observed with trastuzumab treatment. However, if Siglec receptors were not blocked, AbLecs potentiated *in vitro* macrophage phagocytosis (**Fig. 4d**) and NK cell cytotoxicity (**Fig. 4e**). We observed the same evidence of Siglec dependence in HER2+ K562 cells (**Supplemental Fig. 11**). Pretreatment of target cells with sialidase to disrupt

Siglec ligands also abolished AbLec-mediated enhancement of PMN cytotoxicity over trastuzumab (**Supplemental Fig. 10b, c**). Together, these results suggest that the increased levels of phagocytosis and cytotoxicity observed with AbLec treatment are a direct result of glycan blockade.

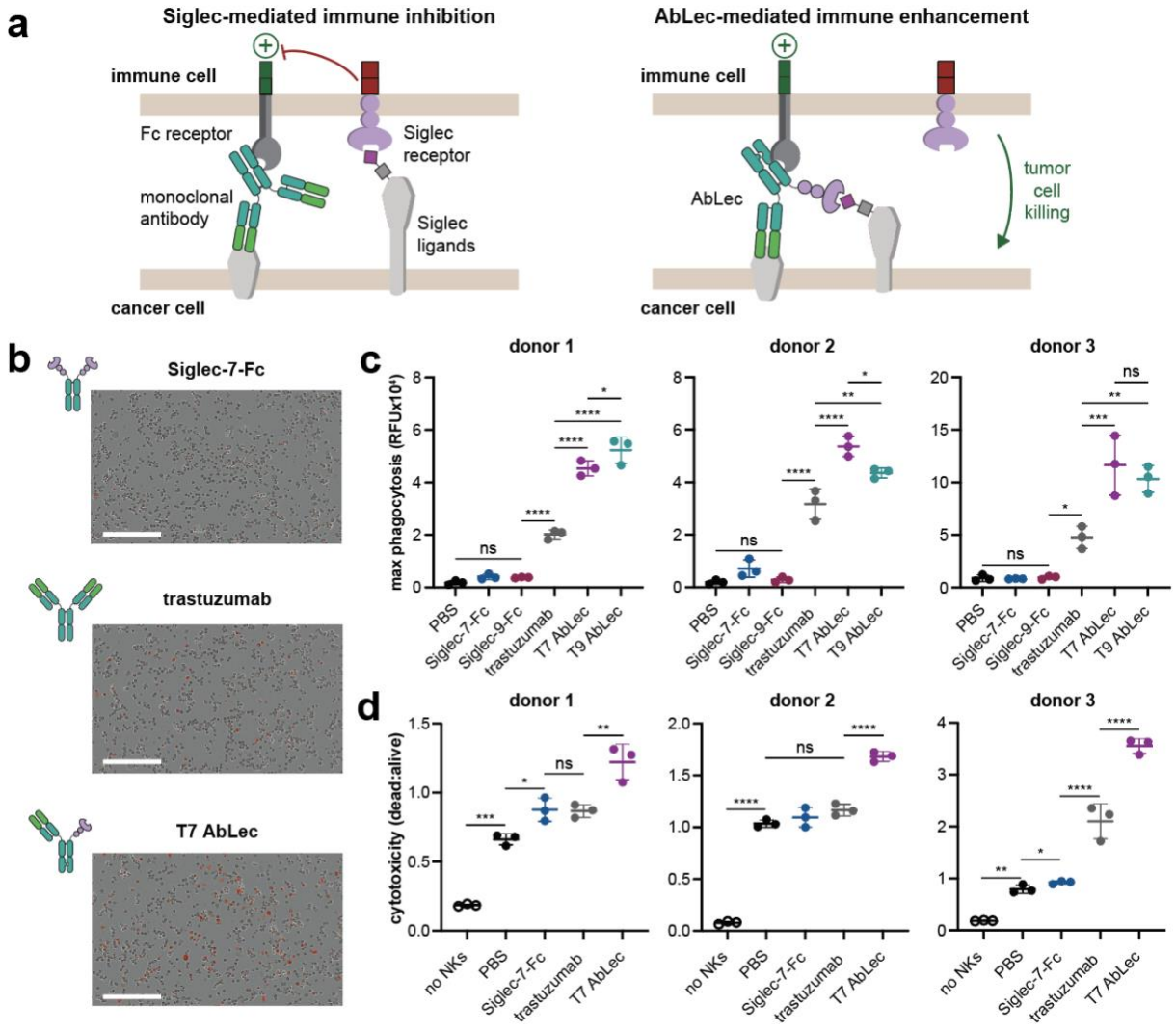

Figure 3. AbLecs potentiate tumor killing *in vitro* via macrophage phagocytosis and NK cell cytotoxicity.

(**a**) Siglec engagement at immune synapses restrains anti-tumor immune responses. We hypothesize that AbLecs recruit immune cells to tumors and simultaneously block Siglec engagement, relieving inhibitory signaling and potentiating tumor killing.

(**b**) Phase contrast and fluorescence microscopy images of macrophage/SK-BR-3 cell co-cultures treated with Siglec-7-Fc, trastuzumab, or T7 AbLec at t = 5 h. SK-BR-3 cells were stained with the pHrodo red pH

sensitive dye which fluoresces upon SK-BR-3 phagocytosis by macrophages. Images are representative of n = 3 biological replicates, scale bar represents 400 μm.

(**c, d**) Quantification of (**c**) macrophage phagocytosis or (**d**) NK cell cytotoxicity of HER2+ SK-BR-3 cells using immune cells from n = 3 human donors. Across all donors, T7 and T9 AbLecs significantly enhanced tumor killing compared to trastuzumab and Siglec-Fc controls (n = 3 biological replicates per donor).

AbLecs outperform combination immunotherapy and synergize with CD47 blockade

Combination of monospecific therapies results in enhanced therapeutic efficacy, and is now thought to be required for durable response in most cancer patients[32]. Thus, we sought to benchmark efficacy of AbLecs compared to combination of trastuzumab with existing Siglec blockade reagents. First, we compared AbLec treatment to combination of trastuzumab with Siglec blocking antibodies[26] (**Fig. 4c, bottom**). Encouragingly, in the setting of macrophage phagocytosis (**Fig. 4d**) and NK cell cytotoxicity (**Fig. 4e**), AbLecs elicited enhanced killing of SK-BR-3 cells compared to the combination of trastuzumab with Siglec-7 or -9 antagonist antibodies[26]. We observed the same trends in phagocytosis and cytotoxicity assays with HER2+ K562 cells (**Supplemental Fig. 11**).

We further compared AbLec efficacy to combination of trastuzumab with *Vibrio cholerae* sialidase (**Fig. 4c, bottom**). The *V. cholerae* sialidase cleaves all linkages (α2,3; α2,6; and α2,8) of terminal sialic acid, blocking Siglec engagement via glycan degradation[11,15]. T7 AbLec treatment outperformed combination of trastuzumab with *V. cholerae* sialidase in eliciting NK cell cytotoxicity, and performed comparably in macrophage phagocytosis assays (**Fig. 4b, e**). Together, these results suggest that AbLec-mediated glycan blockade is more effective than lectin receptor blockade and at least as effective as glycan degradation in eliciting antibody effector functions.

Blockade of the checkpoint molecule CD47, a known “don’t eat me” signal, has been previously shown to elicit anti-tumor immune responses in cancers that otherwise resist treatment with trastuzumab[33]. Thus, we asked whether CD47 blockade synergizes with AbLec treatment to

further enhance tumor phagocytosis (**Fig. 4f**). Indeed, in 2 of the 3 donors tested, combination of CD47 blockade and T7 AbLec elicited enhanced tumor killing compared to AbLec treatment alone (**Fig. 4g**). In all cases, CD47 blockade + AbLec treatment outperformed trastuzumab + CD47 blockade. Combination of CD47 blockade and AbLec therapy also enhanced PMN cytotoxicity over CD47 blockade + trastuzumab (**Supplemental Fig. 10d**). Our results indicate that glyco-immune checkpoint blockade has the potential to synergize with existing immunotherapies possessing distinct, yet complementary, mechanisms of action.

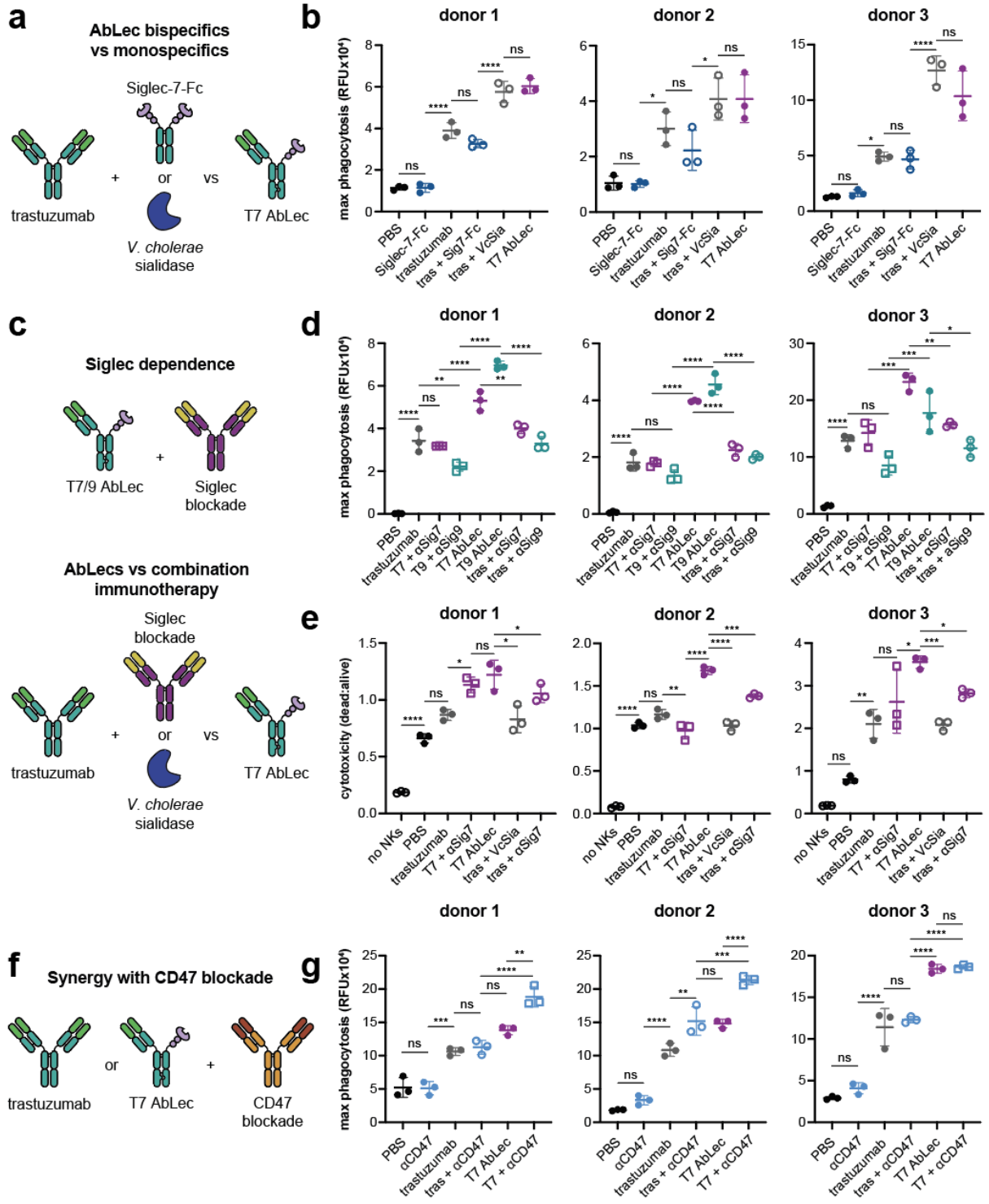

Figure 4. AbLecs function via glyco-immune checkpoint blockade, match or outperform efficacy of combination immunotherapy, and synergize with CD47 blockade.

(**a**) We compared combination of trastuzumab with Siglec-7-Fc or *V. cholerae* sialidase (*Vc*Sia) to T7 AbLec treatment alone in macrophage phagocytosis assays.

(**b**) Quantification of phagocytosis of HER2+ K562 cells using macrophages from n = 3 human donors. Across all donors, T7 AbLec significantly enhanced tumor killing compared to the combination of trastuzumab and Siglec-7-Fc, There was no significant difference in tumor phagocytosis between T7 AbLec treatment and the combination of trastuzumab and *Vc*Sia (n = 3 biological replicates per donor).

(**c**) Siglec-7 and -9 blocking antibodies were used in macrophage phagocytosis and NK cell cytotoxicity assays to assess (**top**) AbLec mechanism of action and (**bottom**) to compare combination of trastuzumab with Siglec blocking antibodies (αSig7 or αSig9) to T7 or T9 AbLec treatment.

(**d**) In the presence of Siglec-7 or -9 blocking antibodies (αSig7 or αSig9), respectively, phagocytosis of HER2+ SK-BR-3 cells induced by T7 and T9 AbLec treatment was not significantly different from the parent monoclonal antibody, trastuzumab. However, if Siglecs were not blocked, T7 and T9 AbLecs enhanced tumor phagocytosis compared to trastuzumab. This was true for macrophages from n = 3 distinct human donors. Across all donors, T7 and T9 AbLecs significantly enhanced tumor killing compared to combination of trastuzumab and Siglec blocking antibodies (n = 3 biological replicates per donor).

(**e**) In the presence of Siglec-7 blocking antibody (αSig7), NK cell cytotoxicity of HER2+ SK-BR-3 cells induced by T7 AbLec treatment was not significantly different from the parent monoclonal antibody, trastuzumab. However, if Siglec-7 was not blocked, T7 AbLec enhanced tumor killing compared to trastuzumab. This was true for NK cells from n = 3 distinct human donors. We also compared combination of trastuzumab with Siglec-7 blocking antibody (αSig7) or *V. cholerae* sialidase (*Vc*Sia) to T7 AbLec treatment alone in NK cell cytotoxicity assays. T7 AbLec treatment outperformed the combination of trastuzumab and Siglec-7 blocking antibody or *Vc*Sia in eliciting NK cell cytotoxicity (n = 3 biological replicates per donor).

(**f**) We tested whether T7 AbLec treatment synergized with CD47 blockade in macrophage phagocytosis assays.

(**g**) Quantification of phagocytosis of HER2+ SK-BR-3 cells using macrophages from n = 3 human donors. In 2 of the 3 donors, T7 AbLec synergized with CD47 blockade. Across all donors, T7 AbLec + CD47 blockade enhanced tumor killing compared to trastuzumab + CD47 blockade (n = 3 biological replicates per donor).

The AbLec approach is applicable to diverse cancer antigens and glycan targets

Due to the modular architecture of the knobs-into-holes bispecific scaffold we employed, AbLecs can be made with a variety of tumor antigen and glycan specificities. To demonstrate this modularity, we constructed AbLecs with components derived from rituximab x Siglec-7 (R7) and cetuximab x Siglec-7 (C7), designed to block Siglec-7-binding glycans on CD20+ and EGFR+ cancer cells, respectively (**Fig. 5a, b**). In addition, we generated a trastuzumab x Siglec-10 AbLec that simultaneously targets HER2+ tumors while blocking ligands of Siglec-10, which was recently shown to play roles in immune evasion in breast and ovarian cancers[14] (**Fig. 5c**). Given our finding that Siglec and CD47 blockade are synergistic (**Fig. 4g**), we designed a magrolimab x Siglec-7 AbLec for dual checkpoint blockade of CD47 and Siglec-7 ligands on tumor cells (**Fig. 5d**). Magrolimab is an anti-CD47 antibody[34] currently in phase III clinical trials for hematological

cancers[35]. Finally, we generated a pembrolizumab x galectin-9 AbLec designed for dual checkpoint blockade of PD-1 and galectin-9 ligands on T cells (**Fig 5e**). Notably, galectin-9 has been shown to facilitate immune evasion by binding the TIM-3 checkpoint receptor on T cells, contributing to CD8+ T cell exhaustion[27,36].

Functional characterization of R7 and C7 AbLecs demonstrated the utility of the AbLec platform for combination tumor targeting and glyco-immune checkpoint blockade in diverse tumor types. Across n = 3 unique donors, R7 and C7 AbLecs significantly enhanced phagocytosis of CD20+ Ramos cells or EGFR+ K562 cells compared to the parent antibody or Siglec-7-Fc alone (**Fig 5f, g; Supplemental Figure 12a**). Importantly, we showed that trastuzumab, rituximab, and cetuximab hybrid AbLecs selectively target antigen expressing cells and spare antigen negative cells (**Supplemental Fig 12**). Further, we found that R7 AbLec treatment enhanced phagocytosis of tumor cells expressing very low levels of the targeted CD20 antigen compared to the parent monoclonal antibody, rituximab (**Supplemental Figure 12c**). Our results demonstrate that AbLecs can be readily engineered to therapeutically target numerous tumor types and glyco-immune checkpoints that play immunosuppressive roles in the tumor microenvironment.

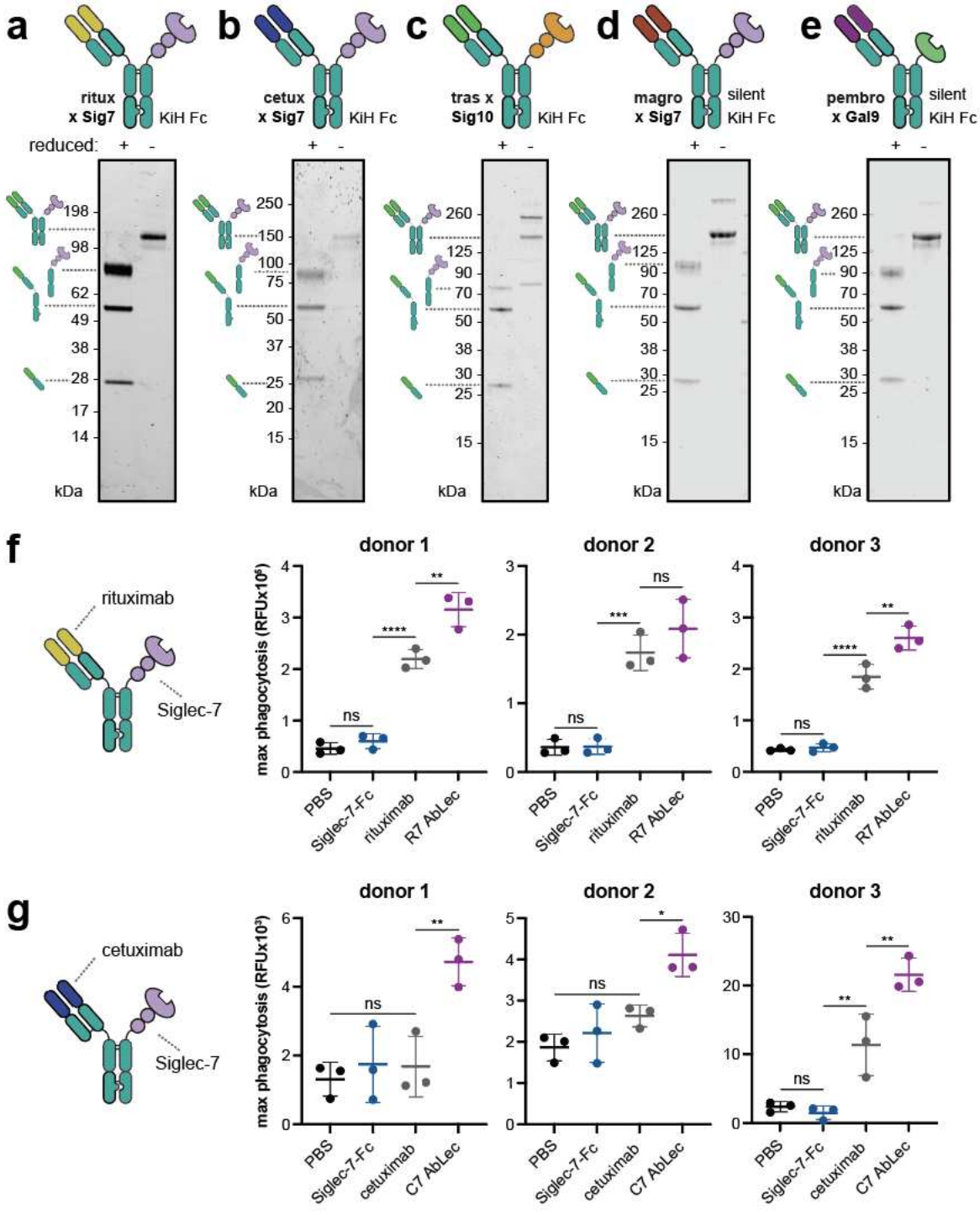

Figure 5. The AbLec platform is modular and can be applied to diverse tumor types and glyco-immune checkpoints.

(**a-e**) Reducing (+) and non-reducing (-) SDS-PAGE analysis of (**a**) rituximab (αCD20) x Siglec-7 (R7) AbLec, (**b**) cetuximab (αEGFR) x Siglec-7 (C7) AbLec, (**c**) trastuzumab (αHER2) x Siglec-10 (T10) AbLec, (**d**) magrolimab (αCD47) x Siglec-7 (M7) AbLec, and (**e**) pembrolizumab (αPD-1) x Galectin-9 (PG9) AbLec. Gels are representative of n = 3 biological replicates.

(**f**) Quantification of phagocytosis of CD20+ Ramos cells using macrophages from n = 3 human donors. Across all donors, R7 AbLec enhanced tumor killing compared to rituximab and Siglec-7-Fc controls (n = 3 biological replicates per donor).

(**g**) Quantification of phagocytosis of EGFR+ K562 cells using macrophages from n = 3 human donors. Across all donors, C7 AbLec enhanced tumor killing compared to cetuximab and Siglec-7-Fc controls (n = 3 biological replicates per donor).

Discussion

In this work, we have established AbLecs as a new class of bispecific molecules for targeted blockade of immunomodulatory glycans for cancer immunotherapy. AbLecs combine high affinity antibodies targeting antigens of interest (e.g., tumor-associated antigens, immune cell markers) with otherwise low affinity glycan binding domains from lectin immunoreceptors. We show that this enables recruitment of glycan binding domains to cell surfaces at therapeutically relevant concentrations and selectively blocks binding of the targeted lectin receptor. AbLec-mediated glyco-immune checkpoint blockade translated into enhanced tumor cell killing by primary human macrophages, NK cells, and PMNs *in vitro* and synergized with CD47 blockade. Overall, AbLecs represent a plug-and-play molecular architecture for direct glycan blockade as a unique immunotherapeutic mechanism of action.

Unexpectedly, we found that Siglec checkpoint blockade with T7 or T9 AbLecs outperformed combination of the parent antibody with Siglec-7 or -9 receptor blocking antibodies in phagocytosis and NK cell cytotoxicity assays. This result suggests that proximity of the tumor targeting and Siglec blockade elements may be important. Specifically, we hypothesize that the ability to block Siglec engagement at the same immune synapse formed by the tumor targeting antibody results in the observed enhanced anti-tumor immunity. Future structure-activity relationship studies will explore the role of proximity of the tumor targeting and glycan binding elements in AbLec efficacy.

We further show that AbLec treatment was at least as effective, if not more effective, than combination of the parent antibody with sialidase. These results support the emerging hypothesis that engagement of Siglec receptors is mediated through the actions of a few high-affinity Siglec

ligands, rather than sialoglycans more broadly[9,14,16,37,38]. This raises the intriguing possibility that using AbLecs to selectively block these professional Siglec ligands can elicit comparable anti-tumor immune responses as those elicited by bulk sialoside degradation. Further studies to uncover the identities of ligands for Siglecs and other glyco-immune checkpoint receptors could enable even more targeted or personalized therapeutic approaches in the future.

Tumors dramatically remodel their cell surface glycosylation[3–5]. It is now clear that a key role for these remodeled glycans is to facilitate immune evasion and tumor progression by engaging multiple broad classes of glycan-binding immunoreceptors, including Siglecs[6], selectins[7], and galectins[8]. AbLecs afford the ability to directly target tumor-associated, immunomodulatory glycans for cancer immunotherapy.

Methods

Plasmids and protein sequences

All AbLec plasmids were generated by Twist Bioscience. DNA sequences are listed in **Supplemental Table 1** and protein sequences in **Supplemental Table 2**. AbLec sequences were inserted into the Twist Bioscience vector pTwist CMV BetaGlobin, using the XhoI and NheI cut sites. The trastuzumab used in this paper was expressed from a pCDNA3.1 vector described in our previous work. The rituximab and cetuximab antibody variable sequences were generated by IDT and cloned into the variable regions of the VRC01 antibody plasmid vector (a generous gift from the Kim lab at Stanford) by using the In-Fusion cloning kit (Takara) according to the manufacturer's protocol.

Protein expression and purification

Antibodies and AbLecs were expressed in the Expi293F system (Thermo Fisher) and expressed according to established manufacturer protocol. For the rituximab and cetuximab antibodies, a

1:1 heavy to light chain plasmid ratio by weight was used. For the AbLecs, a 2:1:1 ratio of lectin:heavy chain:light chain was used. The trastuzumab antibody heavy chain and light chain were co-expressed from a single plasmid. After seven days of expression, proteins were collected from the supernatant by pelleting cells at 300 *x g* for 5 min, followed by clarification with a spin at 3700 *x g* for 40 min, and filtration through a 0.2 µm nylon filter (Fisher Scientific 0974025A). Antibodies were purified by manual gravity column using protein A agarose (Fisher Scientific 20333) by flowing the clarified supernatant through the column 2x, sialidase treating on the beads with 2 µM ST sialidase for 0.5-2 h rt, then washing with 5x column volumes of PBS, and eluting 5 mL at a time with 100 mM glycine buffer pH 2.8 into tubes pre-equilibrated with 150 uL of 1 M Tris pH 8. Antibodies were buffer exchanged into PBS using PD-10 columns (GE). AbLecs were purified by manual gravity column using nickel-NTA agarose resin (Qiagen 30210). Briefly, AbLec supernatant was incubated with the resin (pre-equilibrated in PBS) for ~ 1 hour at 4 C. Beads and supernatant were then loaded onto a chromatography column (BioRad 7321010), sialidase treated on the beads with 2 µM ST sialidase for 2 h rt, washed with 20x column volumes PBS + 20 mM imidazole, and eluted twice with 5x column volumes PBS + 250 mM imidazole. AbLecs were buffer exchanged into PBS using PD-10 desalting columns.

Expression and dye labeling of Siglec-Fc reagents

Siglec-Fc DNA sequences were expressed in Expi293F cells that co-express stable human FGE protein for aldehyde tagging. Cells were expressed in the dark according to the Expi293 protocol from Thermo Fisher, then filtered through a 0.2 µm filter and loaded onto a column containing protein A agarose beads. Protein was sialidase-treated on the column for 2 h (2 µM *Salmonella typhimurium* sialidase, rt). Followed by washing with PBS and elution with 100 mM glycine (pH 2.8), 10 mL, into buffered Tris pH 8 solution. Siglecs were buffer exchanged into acidic buffer, concentrated, and conjugated with HIPS-azide according to the protocol from Gray, *et al*[15]. Siglec-Fc-azide was then taken without further characterization, buffer exchanged into PBS, and 100x

molar equivalents of DBCO-AF647 (Click Chemistry Tools, 1302-1) in DMSO were added and the reaction was mixed at 500 rpm in the dark for 2 hours rt. Siglecs were buffer exchanged by 6x centrifugation on Amicon columns (30 kDa MWCO) in PBS, and AF647 addition was confirmed by using a NanoDrop spectrophotometer at 650 nm for the AF647 dye (extinction coefficient 239,000) and at 280 nm for the protein (using extinction coefficients calculated for each Siglec by Expasy).[18]

AbLec gel characterization

For SDS-PAGE gels, 2 µg of protein with SDS dye alone (non-reducing conditions), or SDS dye + 1 M betamercaptoethanol, heated at 95 C for 5 min (reducing conditions), were loaded onto a Bis-Tris 4–12% Criterion™ XT Bis-Tris Protein Gel, 18 well, (Bio-Rad 3450124) and run with XT-MES buffer at 180 V for 40 min. Proteins were stained with Aquastain (Bulldog Bio AS001000) for 10 minutes followed by a 10 minute destain in water. For western blotting of the AbLecs, 0.2 µg of protein was loaded onto an SDS-PAGE gel and run as described above, then the gel was transferred to a nitrocellulose membrane using the Trans-Blot® Turbo™ RTA Midi Nitrocellulose Transfer Kit (Bio-Rad 1704271), 25V, 14 min. The membrane was blocked in blocking buffer (PBS + 0.5% BSA) for 1 hour rt, then stained with Invitrogen HA Tag Polyclonal Antibody (SG77) (Thermo Fisher Scientific 71-5500) and Purified anti-His Tag antibody (BioLegend 652502) for 1 hour in blocking buffer shaking at rt. The membrane was washed 3x in PBST (PBS + 0.1% Tween), followed by staining with secondary antibodies IRDye® 800CW Goat anti-Mouse and IRDye® 680RD Goat Anti-Rabbit (LI-COR) in PBST for 15 minutes shaking at room temp, followed by 3x more washes in PBST. All gels were imaged on an Odyssey® CLx Imaging System (LI-COR).

AbLec melting temperature characterization

SYPRO orange dye (Thermo Fisher), was diluted to make a 25x stock, and 5 uL (final 5x) concentration with the antibodies) was added to 20 uL of AbLec, Siglec-Fc, or antibody at 0.2 mg/mL in PBS to make 25 uL per well in a 96 well qPCR plate. Denaturation of proteins was analyzed in the FRET fluorescence channel in the qPCR by increasing the temperature 0.5 °C every 1 min from 25 °C to 95 °C.

AbLec mass spectrometry characterization

Four micrograms of each AbLec dissolved in PBS were digested with trypsin for proteomic analysis. Samples were incubated for 18 minutes at 55 °C with 5 mM dithiothreitol, followed by a 30-minute incubation at room temperature in the dark with 15 mM iodoacetamide. Trypsin (Promega) was added at a 1:20 w:w ratio and digestions proceeded at room temperature overnight. The following morning, samples were desalted by first quenching the digestion with formic acid to a final pH of ~2, followed by desalting over a polystyrene-divinylbenzene solid phase extraction (PS-DVB SPE) cartridge (Phenomenex, Torrance, CA). Samples were dried with vacuum centrifugation following desalting and were resuspended in 0.2% formic acid in water at 0.5 µg per µL.

Approximately 1 µg of peptide was injected per analysis, wherein peptides were separated over a 25 cm EasySpray reversed phase LC column (75 µm inner diameter packed with 2 µm, 100 Å, PepMap C18 particles, Thermo Fisher Scientific). The mobile phases (A: water with 0.2% formic acid and B: acetonitrile with 0.2% formic acid) were driven and controlled by a Dionex Ultimate 3000 RPLC nano system (Thermo Fisher Scientific). Gradient elution was performed at 300 nL/min. Mobile phase B was held at 0% over 6 min, followed by an increase to 5% at 7 minutes, 25% at 66 min, a ramp to 90% B at 70 min, and a wash at 90% B for 5 min. Flow was then ramped back to 0% B at 75.1 minutes, and the column was re-equilibrated at 0% B for 15 min, for a total analysis time of 90 minutes. Eluted peptides were analyzed on an Orbitrap Fusion Tribrid MS

system (Thermo Fisher Scientific). Precursors were ionized using an EASY-Spray ionization source (Thermo Fisher Scientific) source held at +2.2 kV compared to ground, and the column was held at 40 °C. The inlet capillary temperature was held at 275 °C. Survey scans of peptide precursors were collected in the Orbitrap from 350-1350 m/z with an AGC target of 1,000,000, a maximum injection time of 50 ms, and a resolution of 60,000 at 200 m/z. Monoisotopic precursor selection was enabled for peptide isotopic distributions, precursors of z = 2-5 were selected for data-dependent MS/MS scans for 2 seconds of cycle time, and dynamic exclusion was set to 30 seconds with a ±10 ppm window set around the precursor monoisotope. An isolation window of 1 m/z was used to select precursor ions with the quadrupole. MS/MS scans were collected using HCD at 30 normalized collision energy (nce) with an AGC target of 100,000 and a maximum injection time of 54 ms. Mass analysis was performed in the Orbitrap a resolution of 30,000 at 200 m/z and scan range set to auto calculation.

Raw data were processed using Byonic[19], version MaxQuant version 3.11.3. Oxidation of methionine (+15.994915) was set as a common[20] variable modification, protein N-terminal acetylation (+42.010565) and asparagine deamination (+0.984016) were specified as rare1 variable modifications, and carbamidomethylation of cysteine (+57.021464) was set as a fixed modification. Up to three common and two rare modifications were permitted. A precursor ion search tolerance of 10 ppm and a product ion mass tolerance of 20 ppm were used for searches, and three missed cleavages were allowed for full trypsin specificity. Peptide spectral matches (PSMs) were made against custom FASTA sequence files that contained appropriate combinations of Siglec-7 and -9 holes, and Trastuzumab/rituximab knobs and light chains. Peptides were filtered to a 1% false discovery rate (FDR) and a 1% protein FDR was applied according to the target-decoy method.2 All peptide identifications were manually inspected, and sequences coverages were calculated only from validated peptide identifications. Sequence

coverage percentages are derived from the proportion of amino acids explained by peptide identifications relative to the total number of amino acids.

Cell culture

All cell lines were purchased from the American Type Culture Collection (ATCC). SK-BR-3, HCC-1954, K562, Raji, and Ramos were cultured in RPMI + 10% heat-inactivated fetal bovine serum (FBS) without antibiotic selection. Expi293F cells were a gift from the Kim lab at Stanford and were cultured according to Thermo Fisher Scientific's user guide. K562s were transfected according to manufacturer's protocol with EGFR using pre-packaged lentiviral particles (G&P Biosciences) and selected for EGFR expression by culture in 1 µg/mL puromycin (InVivoGen). K562s were transfected according to manufacturer's protocol with CD20 using pre-packaged lentiviral particles (G&P Biosciences LTV-CD20) and sorted for CD20-expression using rituximab and a BV421-labeled anti-human secondary (Biolegend) as the staining reagent on a FACS instrument. HER2 WT was a gift from Mien-Chie Hung (Addgene plasmid #16257) and stable $HER2^+$ cell lines were generated following their protocol,[21] protein expression was verified by flow cytometry. Cell lines were not independently authenticated beyond the identity provided from the ATCC. Cell lines were cultivated in a humidified incubator at 5% CO_2 and 37 ºC and tested negative for mycoplasma quarterly using a PCR-based assay.

Quantifying AbLec binding and K_D

HER2+ K562 and SK-BR-3 cells were isolated from the cell culture supernatant or via dissociation with TrypLE (Gibco), respectively, washed with 1xPBS, and resuspended in blocking buffer. 60,000 cells were then distributed into wells of a 96-well V-bottom plate (Corning). Various concentrations (200-0.4 nM) of trastuzumab, Siglec-Fcs, or AbLecs were added to the cells in equal volumes and incubated with cells for 1 h at 4 °C with periodic pipet mixing. Cells were washed three times in blocking buffer, pelleting by centrifugation at 300*g* for 5 min at 4 °C between

washes. Cells were resuspended in AF647 Goat Anti-Human (BioLegend) in blocking buffer for 30 min at 4 °C. Cells were further washed twice and resuspended in blocking buffer, and fluorescence was analyzed by flow cytometry (BD LSR II). Gating was performed using FlowJo v.10.0 software (Tree Star) to eliminate debris and isolate single cells. Mean fluorescence intensity (MFI) of the cell populations were normalized to the MFI of cells stained with 50 nM trastuzumab from each experimental replicate. MFI values were fit to a one-site total binding curve using GraphPad Prism 9, which calculated the K_D values as the antibody concentration needed to achieve a half-maximum binding.

Computational modeling of AbLec binding and apparent ligand concentrations

The *MVsim* multivalent simulation application (version 2021a) was used to model trastuzumab, T7 AbLec, and T7A AbLec binding to HER2+ K562 cells, as previously reported[31]. *MVsim* models the effects of molecular valency, topology, affinity, and kinetics on the binding dynamics of multivalent and multispecific macromolecular receptor-ligand systems. Here, the *MVsim* application was used to create a modeling routine that simulated, via the microstate binding model,[27] the interaction of antibodies and antibody-like chimeras to surfaces populated with specific targeted ligands/antigens. The designed sequences and structures of the biomolecules were used to parameterize the model with the binding valencies. The designed reference biomolecules (e.g., T7A AbLec, Siglec-Fcs) were used to experimentally parameterize the model with monovalent binding affinities. The parameterized model was then used to fit the flow cytometry-based experimental binding data for the apparent concentration ($[C_{app}]$) parameters that derive from the spatial, nearest-neighbor proximity of pairs of targeted cell surface ligands/antigens. Model-derived estimates of $[C_{app}]$ for various designed topologies were interpreted as quantitative assessments of the relative probability or favorability of a candidate therapeutic engaging with a particular cell surface in an advantageous bivalent, and high-avidity interaction.

Competitive binding with Siglec-Fc-AF647 reagents

HER2+ K562 cells were isolated from the cell culture supernatant, washed with 1xPBS, and resuspended in blocking buffer. Cells were aliquoted for sialidase treatment with 100 nM *V. cholerae* sialidase at 37 °C for 30 min in blocking buffer. 60,000 untreated or sialidase treated cells were then distributed into wells of a 96-well V-bottom plate (Corning). Various concentrations (100-0.4 nM) of trastuzumab or AbLecs with 200 nM Siglec-Fc-AF647 reagents were added to the cells in equal volumes and incubated with cells for 2-3 h at 4 °C with periodic pipet mixing. Cells were washed three times and resuspended in blocking buffer, pelleting by centrifugation at 300*g* for 5 min at 4 °C between washes, and fluorescence was analyzed by flow cytometry (BD LSR II). Gating was performed using FlowJo v.10.0 software (Tree Star) to eliminate debris and isolate single cells. Mean fluorescence intensity (MFI) of the cell populations were normalized to the MFI of cells stained with 200 nM Siglec-Fc-AF647 without antibody or AbLecs from each experimental replicate.

Isolation and differentiation of donor macrophages

LRS chambers were obtained from healthy anonymous blood bank donors and PBMCs were isolated using Ficoll-Paque (GE Healthcare Life Sciences) density gradient separation. Monocytes were isolated by plating ~1x10^8 PBMCs in a T75 flask of serum-free RPMI for 1-2 hours, followed by 3x rigorous washes with PBS +Ca +Mg to remove non-adherent cells. The media was then replaced with IMDM with 10% Human AB Serum (Gemini), to differentiate the macrophages for 7-9 days prior to their use in a phagocytosis or flow cytometry experiment.

Macrophage flow cytometry

Macrophages on day 7-9 were lifted from the plate as described above, then fixed for 15 min with 4% formaldehyde (Thermo) in PBS, and washed 3x in PBS and stored at 4 ºC for 2-7 days until

analysis. On the day of analysis, macrophages were stained with CD11b, CD14, Siglecs -7, -9, -10, and an isotype control in blocking buffer for 30 min at 4 ºC. After 2x washes in PBS, macrophages were analyzed by flow cytometry on an LSR II instrument and gated for CD11b and CD14 double positive cells using FlowJo v10. Macrophages were >85% pure by flow cytometry.

Phagocytosis assays

Macrophages were washed with PBS and lifted by 20 min incubation at 37 ºC with 10 mL TrypLE (Thermo). RPMI + 10% HI FBS was added to equal volume, and the macrophages were pelleted by centrifugation at 300 *x g* for 5 min and resuspended in IncuCyte medium (phenol-red free RPMI + 10% HI FBS). Macrophages (10,000 cells, 100 µL) were added to a 96 well flat-bottom plate (Corning) and incubated in a humidified incubator for 1 h at 37 ºC. Meanwhile, target cells were washed 1x with PBS, then treated with 1:80,000 diluted pHrodo red succinimydyl ester dye (Thermo Fisher) in PBS at 37 ºC for 30 min, washed 1x and resuspended in IncuCyte medium. Finally, 10 uL of 20x antibody or AbLec stocks in PBS were added to the macrophages, followed by the pHrodo red-stained target cells (90 uL, 20,000 cells). Antibodies, Siglec decoy receptors, and AbLecs were added at 25 nM, Siglec-7 and -9 blocking antibodies (1E8 and mAbA clones, respectively)[26] were used at 25 µg/mL, *V. cholerae* sialidase was used at 100 nM, and CD47 blocking antibody B6H12[38] was added at 10 µg/mL unless otherwise noted. Cells were plated by gentle centrifugation (50 *x g*, 2 min). Two images per well were acquired at 1 h intervals until the maximum signal was reached (5 hours for breast cancer cell lines and K562 cells, 2 hours for Raji and Ramos cells). The quantification of pHrodo red fluorescence was empirically optimized for phagocytosis of each cell line based on their background fluorescence and size. K562s were analyzed with a threshold of 0.8, an edge sensitivity of -70, and the area was gated to between 100 and 2000 µm^2 with integrated intensities between 300 and 2000 RCU x µm^2 / image. HCC-1954 were analyzed with a threshold of 1.5, an edge sensitivity of -45, and an area between 30 and 2000 µm^2. SK-BR-3 analysis had a threshold of 1, an edge sensitivity of -55, a minimum

integrated intensity of 60, and a maximum area and eccentricity 3000 and 0.96, respectively. Ramos and Raji gating was defined using a threshold of 1.5, an edge sensitivity of -45, and areas between 100 and 2000 μm^2. The total red object integrated intensity (RCU × μm^2/Image) was taken for each image. For each experiment, the maximum phagocytosis measured by pHrodo red was normalized to 1, and then triplicate technical well replicates were averaged for each biological replicate. Replicates from three unique blood donors were plotted in Prism 9.0 (GraphPad Software, Inc).

Isolation of donor NK cells

PBMCs were isolated from LRS chambers as described above, and stocks were prepared at 2-4x10^7 cells in 90% heat-inactivated FBS + 10% DMSO and stored in liquid nitrogen vapor until use. The day prior to use stocks were thawed, NK cells were isolated using the EasySep NK isolation kit (StemCell Technologies 17955), and cells were cultured overnight with 0.5 µg/mL recombinant IL-2 (Biolegend 589106) in RPMI + 10% heat-inactivated FBS until use.

NK cell flow cytometry

Following 24 h activation with IL-2, NK cells were collected from culture supernatant, washed with 1xPBS and resuspended in blocking buffer. On the day of analysis, macrophages were stained with anti-CD16, Siglec-7, and isotype controls in blocking buffer for 30 min at 4 ºC. After 2x washes in PBS, NK cells were analyzed by flow cytometry (BD LSR II) and gated for CD16 positive cells using FlowJo v10. NK cells were >85% pure by flow cytometry.

NK cell killing assays

Target cells were lifted stained with celltracker deep red dye according to manufacturer's protocol. NK cells and target cells were mixed at an effector to target (E/T) ratio of 4:1 and Sytox Green (Thermo) was added at 100 nM. Antibodies, Siglec decoy receptors, and AbLecs were added at

25 nM, Siglec-7 and -9 blocking antibodies (1E8 and mAbA clones, respectively)[26] were used at 25 µg/mL, and *V. cholerae* sialidase was used at 100 nM, unless otherwise noted. Cell death was analyzed by flow cytometry by selecting the red (FL4-A$^+$) cells and calculating the percent dead as Sytox Green$^+$ / total red cells. Replicates from three unique blood donors were plotted in Prism 9.0 (GraphPad Software, Inc).

Isolation of human PMNs

Polymorphonuclear granulocytes (PMN) were isolated from peripheral blood of healthy donors by density gradient centrifugation using either Polymorphprep® (Progen, Heidelberg, DE), as previously described[39]. Isolated PMNs were >82% pure by flow cytometry.

PMN ADCC assays

PMN-mediated ADCC was analyzed in chromium-51 [^{51}Cr] release assays as previously described[40]. AbLecs and antibodies were added at varying concentrations. The CD47 blocking antibody hu5F9-IgG2σ was applied at 20 µg/ml. Effector cells and ^{51}Cr-labelled target cells were added at a ratio of 40:1. After 3 h at 37°C, ^{51}Cr release was measured in counts per minute (cpm) in a MikroBetaTrilux 1450 liquid scintillation and luminescence counter (PerkinElmer, Rodgau Jügensheim, DE). Maximal ^{51}Cr release was achieved by addition of 2% v/v Triton-X 100 solution, while basal ^{51}Cr release was measured in the absence of antibodies. Specific tumor cell lysis in % was calculated as follows:

$$lysis\ [\%] = (experimental\ cpm - basal\ cpm)/(maximal\ cpm - basal\ cpm) \times 100$$

Cell growth and toxicity assays

GFP$^+$ SK-BR-3, HER2$^+$ K562, and HCC-1954 cells were lifted with 2 mL trypsin for 5 min at 37 ºC, rinsed with 8 mL normal growth media and cells were pelleted by centrifugation at 300 *x g* and resuspended in phenol-red-free growth medium containing 50 nM Sytox green cell dead stain

(Thermo Fisher) or 5 nM Sytox red dead cell stain (Thermo Fisher) for the GFP-positive SK-BR-3 line to measure cytotoxicity. Cells were plated onto a flat-bottomed 96 well plate (10,000 cells per well, 95 uL), then 5 uL of AbLec, Siglec, or antibody in PBS was added and mixed, followed by centrifugation at 30 *x g* for 1 min. Images were acquired every 2 h for 3 days. SK-BR-3 cells were analyzed by phase with segmentation adjustment = 1, and a minimum area of 200 μm^2, cell death was quantified by red fluorescence using a threshold of 0.3 RCU, with an edge sensitivity of -50 and areas between 50 and 1000 square microns. HCC-1954 cells had a 0.9 segmentation adjustment, 300 square micron hole-fill, and a minimum area of 200 sq. microns. Sytox green death events were detected with a threshold of 1, an edge sensitivity of -45, and areas between 100-3000 square microns. K562 phase segmentation adjustment was 0.2, with no hole-fill and a minimum area of 60 microns. In the green fluorescence channel, the threshold was 2, with an edge sensitivity of -45 and areas between 50 and 800 microns with eccentricity and integrated intensities less than 0.95 and 40000, respectively.

Acquisition of IncuCyte images

For phagocytosis and toxicity assays, images were obtained over time using an Incucyte® S3 Live-Cell Analysis System (Essen BioScience) within a Thermo Fisher Scientific tissue culture incubator at maintained 37 °C with 5% CO_2. Data were acquired from a 10x objective lens in phase contrast, a green fluorescence channel (ex: 460 ± 20, em: 524 ± 20, acquisition time: 300 ms), and from a red fluorescence channel (ex. 585 ± 20, em: 665 ± 40, acquisition time: 400 ms). Two images per well were acquired at intervals. Unless otherwise specified, all cells were analyzed by Top-Hat segmentation with 100 μm radius, edge split on, hole fill: 0 μm^2.

Statistical Analysis

Statistical analysis was performed in Prism (version 9). For binding curves, one-site-specific binding curves were used to calculate the dissociation constants of antibodies and AbLecs. In

binding assays, NK cell cytotoxicity experiments, phagocytosis experiments, and Siglec expression analyses, ordinary one-way ANOVAs were performed with Tukey's multiple comparison's test to compare treatment groups. In every instance the asterisk * indicates a $p<0.05$, ** indicates $p<0.01$, *** indicates $p<0.001$, and **** indicates $p<0.0001$.

Acknowledgements

J.C.S. acknowledges support from NIH/NCI F32 Postdoctoral Fellowship 1F32CA250324-01, American Cancer Society Postdoctoral Fellowship PF-20-143-01-LIB, and a Sarafan ChEM-H Postdocs at the Interface seed grant. S.W. is supported by funding from the Canadian Institutes of Health Research, the Natural Sciences and Engineering Research Council of Canada, the Cancer Research Society and the Canadian Glycomics Network (GlycoNet). N.M.R. acknowledges support from NIH grant K99GM147304. C.A.S. acknowledges support from NIH (R35 GM136309). C.R.B. acknowledges support from NIH (R01 GM058867-23 and U01 CA226051-02) and a Merck Research Labs Discovery Biologics SEEDS grant.

Author Contributions

J.C.S., M.A.G., S.P.W., and C.R.B. conceived the study. J.C.S., M.A.G., S.P.W., I.I.B., N.M.R., M.K.R, M.L., W.J.E., and B.B. designed and performed experiments and analyzed data. C.A.S., J.V.R., T.V., and C.R.B. directed research and aided in data analysis. J.C.S., M.A.G., and C.R.B. wrote the manuscript. All authors reviewed and/or revised the manuscript.

Conflict of Interest Statement

A patent application relating to antibody-decoy receptor chimeras has been filed by Stanford University (docket no. PCT/US2022/023166). C.R.B. is a co-founder and scientific advisory board member of Lycia Therapeutics, Palleon Pharmaceuticals, Enable Bioscience, Redwood

Biosciences (a subsidiary of Catalent), OliLux Bio, Grace Science LLC, and InterVenn Biosciences.

References

1. Haslam, A. & Prasad, V. Estimation of the Percentage of US Patients With Cancer Who Are Eligible for and Respond to Checkpoint Inhibitor Immunotherapy Drugs. *JAMA Netw Open* **2**, e192535 (2019).
2. Schachter, J. *et al.* Pembrolizumab versus ipilimumab for advanced melanoma: final overall survival results of a multicentre, randomised, open-label phase 3 study (KEYNOTE-006). *Lancet* **390**, 1853–1862 (2017).
3. RodrÍguez, E., Schetters, S. T. T. & van Kooyk, Y. The tumour glyco-code as a novel immune checkpoint for immunotherapy. *Nat. Rev. Immunol.* **18**, 204–211 (2018).
4. Rodrigues Mantuano, N., Natoli, M., Zippelius, A. & Läubli, H. Tumor-associated carbohydrates and immunomodulatory lectins as targets for cancer immunotherapy. *J Immunother Cancer* **8**, (2020).
5. Läubli, H. & Borsig, L. Altered Cell Adhesion and Glycosylation Promote Cancer Immune Suppression and Metastasis. *Front. Immunol.* **10**, 2120 (2019).
6. Smith, B. A. H. & Bertozzi, C. R. The clinical impact of glycobiology: targeting selectins, Siglecs and mammalian glycans. *Nat. Rev. Drug Discov.* **20**, 217–243 (2021).
7. Natoni, A., Macauley, M. S. & O'Dwyer, M. E. Targeting Selectins and Their Ligands in Cancer. *Front. Oncol.* **6**, 93 (2016).
8. Liu, F.-T. & Rabinovich, G. A. Galectins as modulators of tumour progression. *Nat. Rev. Cancer* **5**, 29–41 (2005).
9. Bandala-Sanchez, E. *et al.* T cell regulation mediated by interaction of soluble CD52 with the inhibitory receptor Siglec-10. *Nat. Immunol.* **14**, 741–748 (2013).
10. Laubli, H. *et al.* Engagement of myelomonocytic Siglecs by tumor-associated ligands modulates the innate immune response to cancer. *Proc. Natl. Acad. Sci. U. S. A.* **111**, 14211–14216 (2014).
11. Xiao, H., Woods, E. C., Vukojicic, P. & Bertozzi, C. R. Precision glycocalyx editing as a strategy for cancer immunotherapy. *Proc. Natl. Acad. Sci. U. S. A.* **113**, 10304–10309 (2016).
12. Stanczak, M. A. *et al.* Self-associated molecular patterns mediate cancer immune evasion by engaging Siglecs on T cells. *J. Clin. Invest.* **128**, 4912–4923 (2018).
13. Wang, J. *et al.* Siglec-15 as an immune suppressor and potential target for normalization cancer immunotherapy. *Nat. Med.* **25**, 656–666 (2019).
14. Barkal, A. A. *et al.* CD24 signalling through macrophage Siglec-10 is a target for cancer immunotherapy. *Nature* **572**, 392–396 (2019).
15. Gray, M. A. *et al.* Targeted glycan degradation potentiates the anticancer immune response in vivo. *Nat. Chem. Biol.* **16**, 1376–1384 (2020).
16. Wisnovsky, S. *et al.* Genome-wide CRISPR screens reveal a specific ligand for the glycan-binding immune checkpoint receptor Siglec-7. *Proc. Natl. Acad. Sci. U. S. A.* **118**, (2021).
17. Rodriguez, E. *et al.* Sialic acids in pancreatic cancer cells drive tumour-associated macrophage differentiation via the Siglec receptors Siglec-7 and Siglec-9. *Nat. Commun.* **12**, 1270 (2021).
18. Sterner, E., Flanagan, N. & Gildersleeve, J. C. Perspectives on Anti-Glycan Antibodies Gleaned from Development of a Community Resource Database. *ACS Chem. Biol.* **11**, 1773–1783 (2016).

19. Varki, A. & Angata, T. Siglecs--the major subfamily of I-type lectins. *Glycobiology* **16**, 1r–27r (2006).
20. Pedram, K. *et al.* Design of a mucin-selective protease for targeted degradation of cancer-associated mucins. *bioRxiv* 2022.05.20.492748 (2022) doi:10.1101/2022.05.20.492748.
21. Filipovic, A. *et al.* 482 Phase1/2 study of an anti-galectin-9 antibody, LYT-200, in patients with metastatic solid tumors. *J Immunother Cancer* **9**, (2021).
22. Shum, E. *et al.* 490 Clinical benefit through Siglec-15 targeting with NC318 antibody in subjects with Siglec-15 positive advanced solid tumors. *J Immunother Cancer* **9**, (2021).
23. Dimitriou, F. *et al.* Frequency, Treatment and Outcome of Immune-Related Toxicities in Patients with Immune-Checkpoint Inhibitors for Advanced Melanoma: Results from an Institutional Database Analysis. *Cancers* **13**, (2021).
24. Perez, E. A. *et al.* Incidence of adverse events with therapies targeting HER2-positive metastatic breast cancer: a literature review. *Breast Cancer Res. Treat.* **194**, 1–11 (2022).
25. Haas, Q. *et al.* Siglec-9 Regulates an Effector Memory CD8+ T-cell Subset That Congregates in the Melanoma Tumor Microenvironment. *Cancer Immunol Res* **7**, 707–718 (2019).
26. Ibarlucea-Benitez, I., Weitzenfeld, P., Smith, P. & Ravetch, J. V. Siglecs-7/9 function as inhibitory immune checkpoints in vivo and can be targeted to enhance therapeutic antitumor immunity. *Proc. Natl. Acad. Sci. U. S. A.* **118**, (2021).
27. Jin, H.-T. *et al.* Cooperation of Tim-3 and PD-1 in CD8 T-cell exhaustion during chronic viral infection. *Proc. Natl. Acad. Sci. U. S. A.* **107**, 14733–14738 (2010).
28. Ridgway, J. B., Presta, L. G. & Carter, P. “Knobs-into-holes” engineering of antibody CH3 domains for heavy chain heterodimerization. *Protein Eng.* **9**, 617–621 (1996).
29. Delaveris, C. S., Chiu, S. H., Riley, N. M. & Bertozzi, C. R. Modulation of immune cell reactivity with cis-binding Siglec agonists. *Proc. Natl. Acad. Sci. U. S. A.* **118**, (2021).
30. Errington, W. J., Bruncsics, B. & Sarkar, C. A. Mechanisms of noncanonical binding dynamics in multivalent protein–protein interactions. *Proceedings of the National Academy of Sciences* **116**, 25659–25667 (2019).
31. Bruncsics, B., Errington, W. J. & Sarkar, C. A. MVsim is a toolset for quantifying and designing multivalent interactions. *Nat. Commun.* **13**, 1–13 (2022).
32. Sharma, P. & Allison, J. P. Immune checkpoint targeting in cancer therapy: toward combination strategies with curative potential. *Cell* **161**, 205–214 (2015).
33. Upton, R. *et al.* Combining CD47 blockade with trastuzumab eliminates HER2-positive breast cancer cells and overcomes trastuzumab tolerance. *Proc. Natl. Acad. Sci. U. S. A.* **118**, (2021).
34. Liu, J. *et al.* Pre-Clinical Development of a Humanized Anti-CD47 Antibody with Anti-Cancer Therapeutic Potential. *PLoS One* **10**, e0137345 (2015).
35. Garcia-Manero, G. *et al.* Magrolimab + azacitidine versus azacitidine + placebo in untreated higher risk (HR) myelodysplastic syndrome (MDS): The phase 3, randomized, ENHANCE study. *J. Clin. Orthod.* **39**, TPS7055–TPS7055 (2021).
36. Yang, R. *et al.* Galectin-9 interacts with PD-1 and TIM-3 to regulate T cell death and is a target for cancer immunotherapy. *Nat. Commun.* **12**, 1–17 (2021).
37. Beatson, R. *et al.* The mucin MUC1 modulates the tumor immunological microenvironment through engagement of the lectin Siglec-9. *Nat. Immunol.* **17**, 1273–1281 (2016).
38. Theruvath, J. *et al.* Anti-GD2 synergizes with CD47 blockade to mediate tumor eradication. *Nat. Med.* **28**, 333–344 (2022).
39. Derer, S. *et al.* Increasing FcγRIIa affinity of an FcγRIII-optimized anti-EGFR antibody restores neutrophil-mediated cytotoxicity. *MAbs* **6**, 409–421 (2014).
40. Lohse, S. *et al.* An Anti-EGFR IgA That Displays Improved Pharmacokinetics and Myeloid Effector Cell Engagement In Vivo. *Cancer Res.* **76**, 403–417 (2016).